Published OnlineFirst November 13, 2012; DOI: 10.1158/0008-5472.CAN-12-2220

Cancer Research

MIG-7 Controls COX-2/PGE2-Mediated Lung Cancer Metastasis

Ming-Yi Ho[1], Shu-Mei Liang[1,2], Shao-Wen Hung[2], and Chi-Ming Liang[1,3]

Abstract

More effective treatments for metastatic lung cancer remain a pressing clinical need. In this study, we identified migration inducting gene-7 (MIG-7) protein as critical for COX-2/prostaglandin E2 (PGE2)- and Akt/GSK-3β-dependent tumor invasion/metastasis. COX-2/PGE2 activated EP4 to enhance Akt and GSK-3β phosphorylation and β-catenin/T-cell factor/lymphoid enhancer factor signaling leading to MIG-7 upregulation. RNAi-mediated attenuation of MIG-7 blocked COX-2/PGE2- and Akt/GSK-3β-mediated migration/invasion effects. Furthermore, MIG-7 protein inhibited protein phosphatase 2A to sustain Akt/GSK-3β phosphorylation and cancer-cell migration/invasion. Cancer cells overexpressing MIG-7 exhibited increased expression of ZEB-1 and Twist in parallel with epithelial–mesenchymal transition, metastasis and cancer lethality. MIG-7 protein level positively correlated with advanced stages of human lung cancers. MIG-7 thus offers a theranostic target for cancer metastases arising from aberrant activation of the cellular COX-2/PGE2 and Akt/GSK-3β signaling pathways. *Cancer Res; 73(1); 1–11. ©2012 AACR.*

Introduction

Lung cancer is the leading cause of cancer death worldwide. The major cause of treatment failure and mortality is cancer metastasis (1–3). The cyclooxygenases (COX), key enzymes in the biosynthesis of prostaglandins, are potential mediators of metastasis. Overexpression of COX-2, an inducible form of COX, is frequently found in early and advanced lung cancer tissues and is associated with poor prognosis (4–7). Elevated levels of tumor COX-2 and its metabolite prostaglandin E2 (PGE2) contribute to a decrease in E-cadherin, induction of tumor angiogenesis, augmentation of cancer motility and invasiveness, resistance to apoptosis, and suppression of antitumor immunity (5, 8, 9).

The binding of PGE2 to 1 or more of its 4 G protein-coupled receptors, designated EP1, EP2, EP3, and EP4, has been shown to stimulate phosphatidylinositol 3-kinase/protein kinase B (PI3K/Akt) and extracellular signal-regulated kinase 1/2 (ERK1/2) signaling and is implicated in cancer-cell growth and progression (8–11). However, both the COX-2/PGE2 and PI3K/Akt signaling cascades exist in normal cells with pleiotropic functions and inhibition of these 2 important signaling pathways causes a variety of undesirable side effects (12, 13). One notorious example of the effects of the long-term use of COX-2 inhibitors is rofecoxib (Vioxx) that resulted in renal and cardiovascular system impairment and was withdrawn from the market in 2004 (14, 15). Discovery of agents that target the downstream effector(s) of COX-2/PGE2 and PI3K/Akt signaling cascades is desirable to aid the development of therapeutics that have better selectivity and specificity and no severe adverse effects.

Another potential mediator of metastasis is migration inducting gene-7 (MIG-7) protein (16). Increase in *MIG-7* mRNA is found in embryonic cytotrophoblast cells during placenta development as well as in more than 80% of tumor cells, but not found in 25 different normal tissues or in blood from normal subjects (16–18). Transduction of MIG-7 in carcinoma cells results in invasion by carcinoma cells in 3-dimensional culture *in vitro* (17). Stably expressing *MIG-7*-specific shRNA, on the other hand, reduces phosphorylation of Akt and ERK1/2 and attenuates membrane-type 1 matrix metalloproteinase (MT1-MMP) activity in endometrial carcinoma cell lines (19). Whether or not this holds true for lung cancer has not been examined and functional association between MIG-7 and COX-2/PGE2 signaling in promoting lung cancer invasion/metastasis remains elusive.

In this study, we found that MIG-7 was functionally associated with COX-2/PGE2-induced lung cancer metastasis through phosphorylation of Akt and glycogen sythase kinase-3 β (GSK-3β), activation of β-catenin/TCF-4/LEF-1 signaling and decrease in the activity of protein phosphatase 2A (PP2A). The critical role of MIG-7 protein was further substantiated by examining its level in the human lung cancers as well as the effects of overexpressing MIG-7 on lung cancer cells in a xenograft mouse model.

Materials and Methods

Materials

A549 cell line [American Type Culture Collection (ATCC: CCL-185)], H1299 (ATCC: CRL-5803), CL1-0, and CL1-5 (20)

Authors' Affiliations: [1]Genomics Research Center, [2]Agricultural Biotechnology Research Center, and [3]Institute of Biological Chemistry, Academia Sinica, Taipei, Taiwan, ROC

Note: Supplementary data for this article are available at Cancer Research Online (http://cancerres.aacrjournals.org/).

Corresponding Authors: Chi-Ming Liang, Academia Sinica, Rm 727, ABRC, No. 128, Sec. 2, Academia Road, Taipei 11529, Taiwan. Phone: 8862-2787-2501; Fax: 8862-2651-8049; E-mail: cmliang@gate.sinica.edu.tw; and Shu-Mei Liang, Academia Sinica, Rm 626, ABRC, No. 128, Sec. 2, Academia Road, Taipei 11529, Taiwan. Phone: 8862-2652-2870; E-mail: smyang@gate.sinica.edu.tw

doi: 10.1158/0008-5472.CAN-12-2220

Published OnlineFirst November 13, 2012; DOI: 10.1158/0008-5472.CAN-12-2220

were maintained in Dulbecco's Modified Eagle's Media or RPMI medium (GibcoBRL Life Technologies) supplemented with 10% FBS (GibcoBRL Life Technologies) and 1% penicillin-streptomycin-neomycin (GibcoBRL Life Technologies). A human lung fibroblast cell line (WI-38) was obtained from Abcam. A549 and H1299 cells were certified by the Food Industry Research and Development Institute (Hsinchu, Taiwan) in 2012. *MIG-7* siRNA and scrambled control siRNA were purchased from Dharmacon (Thermo Fisher Scientific). The sequences of the *MIG7-1* siRNA and *MIG7-2* siRNA are: GUCGAAGAAAUGAAACUUUUU and CUUAAAUCACAGGAAAUCUUU. *MIG-7* siRNA transfection was undertaken by using Dharmacon Accell SMARTpool siRNA reagent (Thermo Fisher Scientific) according to the protocol recommended by Dharmacon. The MIG7 shRNA-encoding sequences cloned in pGPU6/Neo siRNA Expression vectors were obtained from GenDiscovery Biotechnology. The *MIG7-1* or *MIG7-2* shRNA encoding sequence was created by using the 2 complementary oligonucleotides indicated below, each containing the 21 nucleotides target sequence of *MIG7* (313–333 or 1523–1543), followed by a short spacer TTCAAGAGA: shMIG7-1 sense, 5′-CACCGCAAGTACAGGGCAGAATTTCTTCAAGAGAGAAATTCTGCCCTGTACTTGCTTTTTTG-3′; shMIG7-1 antisense, 5′-GATCCAAAAAAGCAAGTACAGGGCAGAATTTCTCTCTTGAAGAAATTCTGCCCTGTACTTGC-3′; shMIG7-2 sense, 5′-CACCGCCATCTGTGAGATTACAAATTTCAAGAGAATTTGATATCTCACAGATGGCTTTTTTG-3′; and shMIG7-2 antisense, 5′-GATCCAAAAAAGCCATCTGTGAGATATCAAATTCTCTTGAAATTTGATATCTCACAGATGGC-3′. Mice, antibodies, and other reagents are described on the Supplementary Materials and Methods.

Knockdown and overexpression of proteins

Full-length human *COX-2* cDNA (NM 000963.2) and human *MIG-7* (DQ080207.2) cDNA derived from A549 cells were amplified by using specific primers (Supplementary Table S1; Sigma-Proligo) and subcloned into pcDNA6/BioEase-DEST by Gateway cloning technology (Invitrogen) to generate pCOX-2 plasmids (pCOX2) and pMIG7 plasmids. The insert sequences in the plasmids were confirmed by automated DNA sequencing. The plasmids or siRNAs were transfected into cell lines by PolyJet *In Vitro* DNA Transfection Reagent or GeneMute siRNA and DNA Transfection Reagent (SignaGen laboratories). The expression of target proteins in the transfected cells was determined 48 hours after transfection, unless specified otherwise.

Immunoblotting, immunoprecipitation, and gelatin zymographic analysis

Gelatinolytic activities of MMP-2 and MMP-9, immunoprecipitation, and immunoblotting were conducted as described previously (21, 22).

Migration, invasion, and anchorage-independent growth assays

In vitro migration, invasion, and anchorage-independent growth assays were conducted as described previously (23).

Luciferase reporter assay

To examine transcriptional regulation of *MIG7* promoters, genomic DNA was isolated from the A549 cell line and approximately 3 kb of the *MIG7* promoter was amplified by PCR using the specific primers listed in Supplementary Table S1 (Sigma-Proligo) and subcloned into the pGL3-basic vector (Promega) to generate the *MIG7* promoter/firefly luciferase reporter construct, designated pGL3-*MIG7*. To analyze T-cell factor/lymphoid enhancer factor (TCF/LEF)-dependent promoter activity, we purchased TOPflash (wild-type TCF binding sites reporter plasmid) and FOPflash (nonresponsive mutated TCF binding sites reporter plasmid; Millipore). pRL-TK plasmid (Promega) containing *Renilla* luciferase was used as an internal control. At 24 to 36 hours after transfection, cell lysates were assayed using the Dual-Luciferase Reporter Assay System (Promega) and luciferase activities were measured with a luminometer (Wallac Vector3; PerkinElmer).

PP2A activity assay

Cellular PP2A activity was assayed using a PP2A immunoprecipitation phosphatase assay kit (Upstate) according to the manufacturer's instructions.

Preparation of pCMV-GFP/luciferase-lentivirus and establishment of stable cell lines

$A549^{GL}$ cells were produced by infecting A549 cells with cytomegalovirus promoter (pCMV)-GFP/luciferase-lentivirus as described previously (22). $A549^{GL}$ cells were then transfected with pcDNA6/BioEase-DEST (empty vector; EV) or pMIG7 plasmids and then selected with blasticidin (100 μg/mL) to produce $A549^{EV\text{-}GL}$ and $A549^{MIG7\text{-}GL}$ stable cell lines, respectively. Some $549^{MIG7\text{-}GL}$ cells were transfected with *MIG7-1* short hairpin RNA (shRNA) and then selected with G418 (400 μg/mL) to produce $A549^{MIG7shMIG7\text{-}GL}$ stable cell lines. CL1-$0^{EV\text{-}GL}$, CL1-$0^{MIG7\text{-}GL}$, and CL1-$0^{MIG7shMIG7\text{-}GL}$ stable cell lines were prepared according to the same procedure. In addition, CL1-5^{GL} cells were transfected with control shRNA, *MIG7-1* shRNA, and *MIG7-2* shRNA separately and selected with G418 (400 μg/mL) to produce CL1-$5^{shCont\text{-}GL}$, CL1-$5^{shMIG7\text{-}1\text{-}GL}$, and CL1-$5^{shMIG7\text{-}2\text{-}GL}$ stable cell lines. The expression level of MIG-7 in each stable cell lines was analyzed by immunoblot analysis (Supplementary Fig. S5E).

Experimental xenograft murine metastasis model

Male severe combined immunodeficient mice ($n = 9$/group) were implanted with 50 μL RPMI medium (vehicle) or 1×10^6/50 μL lung tumor cells on day 0 by lateral tail vein injection. Metastatic progression was monitored weekly and quantified using a noninvasive bioluminescence In Vivo Imaging System (IVIS) (Xenogen) as described previously (22). Thirty-five days after injection, 3 mice were killed for necropsy and the other 6 mice were kept for survival studies. The percentage of animal survival in each group was routinely recorded.

Immunohistochemistry, histopathology examination, and assessment of MIG-7 protein level

Human lung carcinoma tissue microarray (TMA) slides were purchased from US Biomax (BC41114) and verified by a

Published OnlineFirst November 13, 2012; DOI: 10.1158/0008-5472.CAN-12-2220

qualified, experienced pathologist (Dr. Wei-Hwa Lee). Immunohistochemistry and histopathology analyses were conducted as described previously (22, 24). The images were scanned into a digital format by Scanscope XT system (Aperio Technologies) and analyzed using Aperio ImageScope 9.1 software (Aperio Technologies). The percentage of positive cells from 5 fields of each tissue sample was scored as follows: 0 (0%–5%), 1 (5%–20%), 2 (20%–40%) and 3 (>40%) of tumor tissue stained. Signal intensity from 5 fields of each tissue sample was scored by their staining color as follows: 0 (no immunostaining), 1 (light brown), 2 (medium brown), and 3 (dark brown). Two scores for each tissue sample were combined to evaluate the relative intensity and expression percentage of MIG-7 in each tissue sample.

Statistics

All statistical comparisons were made with 2-tailed tests. The survival time was assessed using Kaplan–Meier curves and tested for significance by the log-rank test. Statistical evaluation was conducted using GraphPad Prism version 5.0 for Microsoft Windows (GraphPad Software). Differences between groups were considered statistically significant at *, $P < 0.05$; **, $P < 0.01$, or ***, $P < 0.0001$.

Results

MIG-7 protein plays an important role in COX-2-induced migration and invasion of lung cancer cells

MIG-7 protein expressed in A549, H1299, CL1-0, and CL1-5 human lung cancer cell lines (Supplementary Fig. S1A). To examine the potential relationship between COX-2, MIG-7 protein, and cell invasiveness, we treated these lung cancer cells with COX-2-specific inhibitor NS398 or *COX-2* siRNA (siCOX2) and found that it inhibited MIG-7 protein (by 2- to 4.5-fold) and decreased epithelial–mesenchymal transition (EMT) as indicated by a 2- to 4.5-fold increase in the level of epithelial cell marker E-cadherin and a 3- to 4.5-fold decrease in

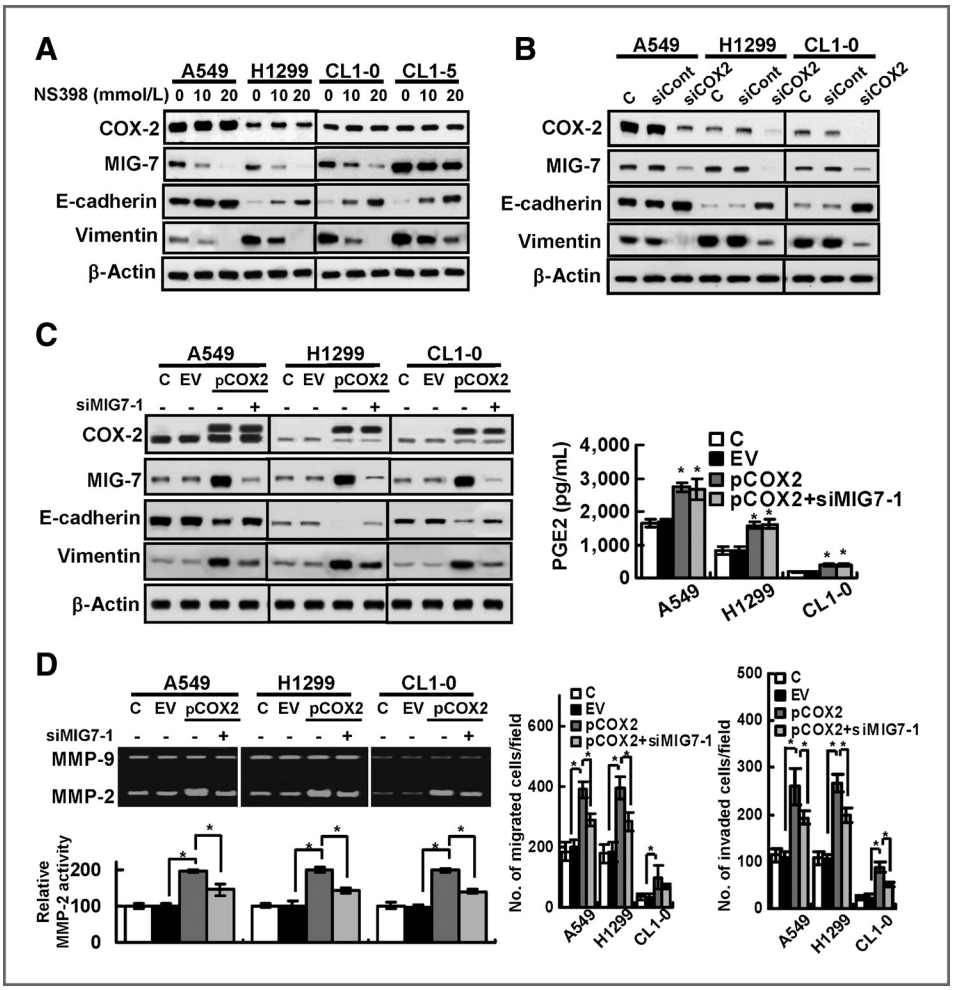

Figure 1. MIG-7 protein is functionally associated with COX-2-mediated upregulation of EMT, MMP-2 activity, and migration/invasion of lung cancer cells. Cells were examined by immunoblotting for protein expression, zymography for MMP activity and transwell assay for cell migration/invasion as described in Materials and Methods. Blots are representative of 3 independent experiments. Data represent means ± SD of 3 independent experiments; *, $P < 0.05$ by *t* test. A and B, lung cancer cells (2×10^5/mL) were treated with COX-2 antagonist NS398 for 24 hours or control scrambled siRNA (siCont) and *COX-2* siRNA(siCOX2) for 48 hours as indicated. C and D, knockdown of MIG-7 suppressed COX-2-mediated effects but not COX-2 or PGE2 level. Parental lung cancer cells (A549, H1299, and CL1-0; C) were transfected with EV, pCOX2, control scrambled siRNAs (-siMIG7-1), or *MIG7-1* siRNAs (+siMIG7-1) for 48 hours as indicated.

Published OnlineFirst November 13, 2012; DOI: 10.1158/0008-5472.CAN-12-2220

the level of mesenchymal cell marker vimentin (Fig. 1A and B). siCOX2 also decreased PGE2, MMP-2 activity, and migration/invasion by 2- to 4.5-fold in lung cancer cells (Supplementary Fig. S1B–S1D). In contrast, overexpressing COX-2 by transfection with pCOX2 increased COX-2 together with MIG-7 protein, PGE2, EMT, MMP-2 activity, and migration/invasion by 2- to 3.5-fold in lung cancer cells (Fig. 1C and D). MIG-7 knockdown (+siMIG7-1 or +siMIG7-2) attenuated the effect of COX-2 overexpression on MIG-7, EMT, MMP-2, and the migration/invasion of the cells by 30% to 60%, but did not affect expression level of COX-2 and PGE2 (Fig. 1C and D, Supplementary Fig. S1E and S1F).

PGE2-mediated EP4/Akt/GSK-3β signaling increases MIG-7 protein level to upregualte EMT and cell migration/invasion

The binding of PGE2 to EP receptors promotes colorectal cancer growth and progression (8, 25). We found that over-expressing COX-2 in lung cancer cells increased intracellular and extracellular PGE2 level by about 2-fold (Supplementary Fig. S2A). The enhancing effects of COX-2 and PGE2 on EMT, MIG-7 protein level, MMP-2 activity, and cancer cell migration/invasion were dependent on EP4 but not EP1 or EP2, as they were completely reversed by treatment of EP4 antagonist AH23848 or *EP4* siRNA (siEP4; Fig. 2A and B, Supplementary Fig. S2B and S2C) but not by treatment of *EP1* siRNA or *EP2* siRNA.

Activation of PGE2-EP4 signaling stimulates the PI3K/Akt and ERK1/2 signaling cascades (8–11, 25). In this study, we found that PGE2 treatment of lung cancer cells for 40 to 60 minutes activated Akt by phosphorylation at serine 473, ERK1/2 by phosphorylation at threonine 185 and tyrosine 187 and inactivated GSK-3β by phosphorylation at serine 9 (Supplementary Fig. S2D). Overexpressing constitutively active Akt with dominant-active Akt plasmids (pAkt-DA) increased MIG-7 protein, EMT, MMP-2 activity, and cell migration and

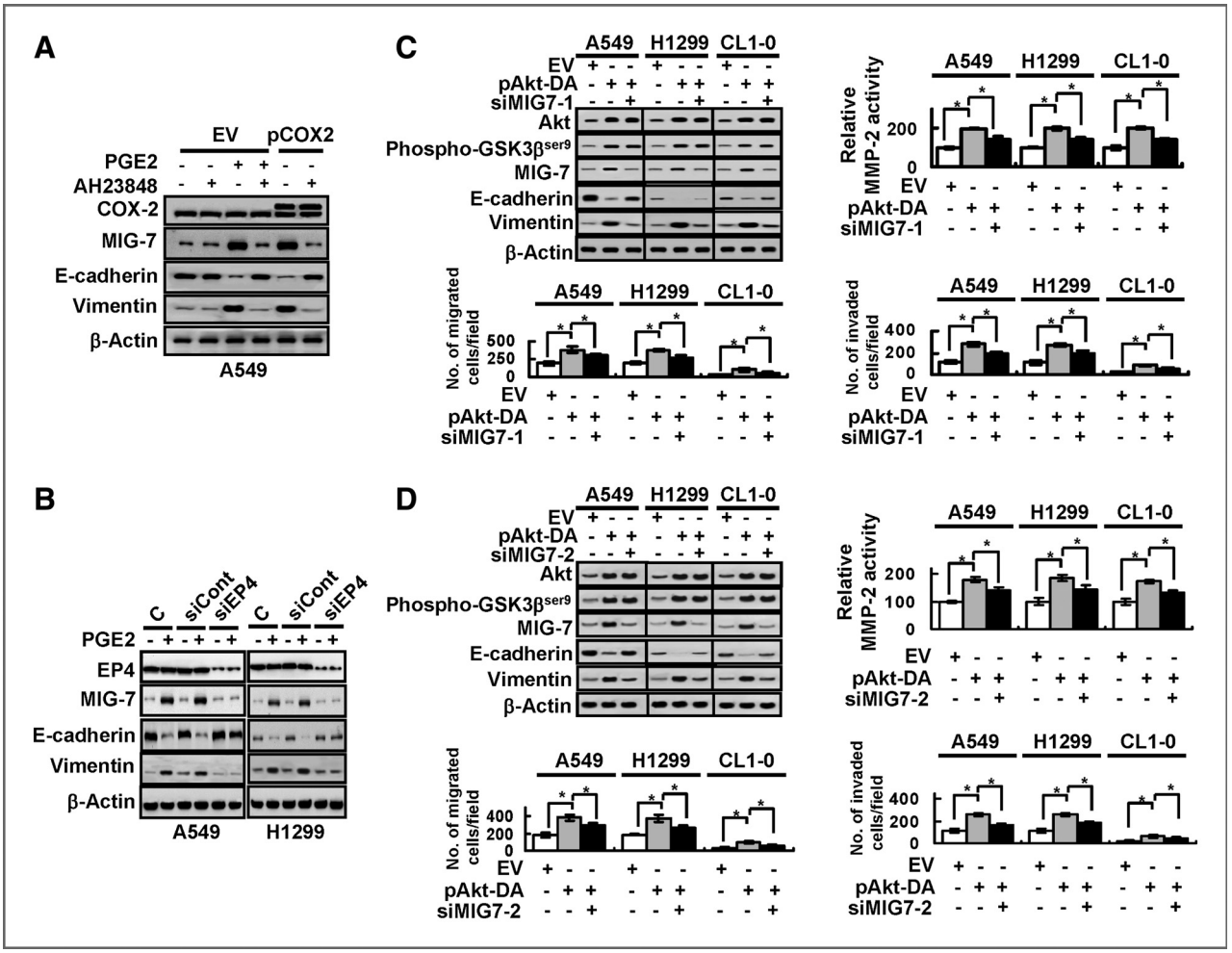

Figure 2. COX-2/PGE2-EP4 signaling phosphorylates Akt and GSK-3β to increase MIG-7 protein and upregulate EMT and cell migration/invasion. A, parental cells (A549; C) transfected with EV or pCOX2 for 48 hours were pretreated with AH23848 (50 μmol/L) for 30 minutes and then treated with PGE2 (20 μg/mL) for 24 hours as indicated. B, lung cancer cells (2×10^5/mL) were transfected with control scrambled siRNA (siCont) or *EP4* siRNA (siEP4) for 48 hours (right) and then treated with PGE2 (20 μg/mL) for 24 hours as indicated. C and D, lung cancer cells (A549, H1299, and CL1-0; C) were transfected with EV, dominant-active Akt (pAkt-DA) plasmids, control scrambled siRNA (-siMIG7-1 and -siMIG7-2), *MIG-7-1* siRNA (+siMIG7-1), and *MIG-7-2* siRNA (+siMIG7-2) as indicated. Blots are representative of 3 independent experiments. Data represent means ± SD of 3 independent experiments; *, $P < 0.05$ by *t* test.

Published OnlineFirst November 13, 2012; DOI: 10.1158/0008-5472.CAN-12-2220

invasion by 2- to 3-fold (Fig. 2C and D). Knockdown of MIG-7 attenuated effects of Akt overexpression on EMT, MMP-2 activity, and cell invasion (by 30%–60%) but not phosphorylation of GSK-3β (Fig. 2C and D), indicating that MIG-7 is the downstream target of Akt/GSK-3β signaling.

Activation of Akt/GSK-3β signaling enhances β-catenin-TCF-4/LEF-1 signaling cascade to elevate MIG-7 protein level

In some cancer cells, inactivation of GSK-3β by phosphorylation at serine 9 has been shown to increase the accumulation of nuclear β-catenin, which associates with TCF/LEF to turn on Wnt signaling (26, 27) and transactivate transcription of target genes (28). To observe whether phosphorylated GSK-3β^{Ser9} causes activation of Wnt signaling in lung cancer cells, we used a luciferase reporter system in which the promoter module contained TCF binding sites (TOPflash) or nonresponsive, mutated binding sites (FOPflash). COX-2 and PGE2 increased the EP4-dependent luciferase activity of TOPflash/FOPflash up to 45-fold that was accompanied with 11-fold increase in *MIG-7* transcription in the lung cancer cells (Supplementary Fig. S3A). We further transfected A549 cells with dominant active (non-phosphorylated S9A-GSK-3β mutant) and dominant negative (kinase-deficient K85A-GSK-3β mutant) plasmids (29) to examine whether they can regulate Wnt signaling and MIG-7 level. Our results showed that constitutive overexpression of active GSK-3β by transfection of *S9A-GSK-3β* plasmids (pGSK3β-DA) downregulated phosphorylation of GSK-3β and attenuated accumulation of β-catenin, TOPflash reporter activity, and MIG-7 expression by 60% to 75% under PGE2 stimulation (Fig. 3A). Transfection of *K85A-GSK-3β* plasmids (pGSK3β-DN), on the other hand, resulted in 2- to 4-fold increase in levels of β-catenin and MIG-7 proteins as well as around 40-fold increase in TOPflash reporter activity in lung cancer cells (Fig. 3A). In addition, increase of β-catenin by transfection of active form of β-catenin (pβ-catenin-S33A) enhanced TOPflash reporter activity by 45-fold and MIG-7 expression more than 2-fold in A549 cells (Fig. 3B). These results showed activation of Wnt signaling and induction of MIG-7 expression by phosphorylated GSK-3β^{Ser9} in lung cancer cells.

Transfection with *TCF-4* plasmids (pTCF4; 0.5–2 μg), *LEF-1* plasmids (pLEF1; 0.5–2 μg), or both pTCF4 and pLEF1

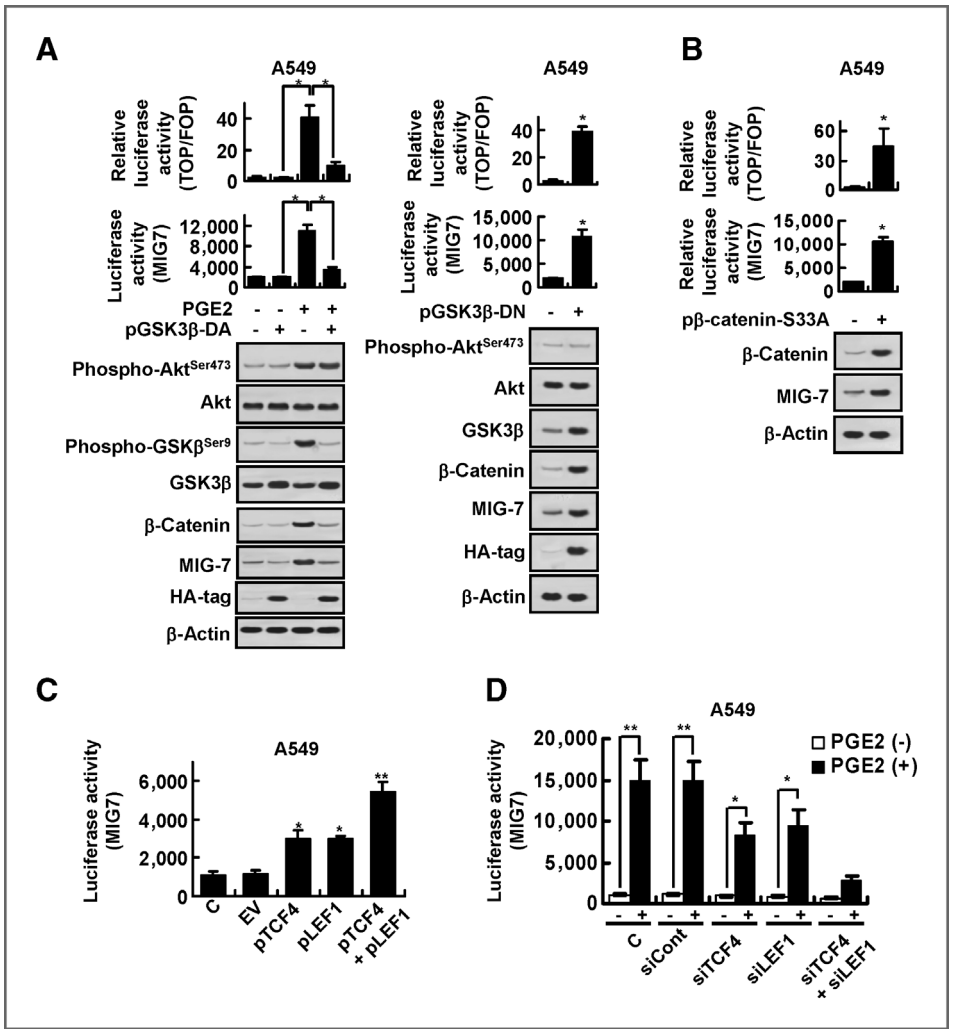

Figure 3. PGE2-mediated transactivation of *MIG7* gene involves a β-catenin-TCF-4/LEF-1 pathway. A and B, parental cells (A549; C) cotransfected with reporter plasmids TOPflash/FOPflash and pRL-TK and plasmids of empty vector (-pGSK3β-DA, -pGSK3β-DN, -pβ-catenin-S33A), dominant-active GSK3β (+pGSK3β-DA), dominant-inactive GSK3β (+pGSK3β-DN), and dominant-active β-catenin (+pβ-catenin-S33A) were treated with or without PGE2 (20 μg/mL) for 24 hours as indicated. C, parental cells (A549; C) were cotransfected with reporter plasmids pGL3-*MIG7* and pRL-TK and plasmids of EV, TCF-4 (pTCF4), *LEF-1* (pLEF1), or a combination of TCF-4 and *LEF-1* plasmids (pTCF4 + pLEF1) for 24 hours as indicated. D, parental cells (A549; C) cotransfected with reporter plasmids pGL3-MIG7 and pRL-TK and control scrambled siRNA (siCont) or *TCF-4* siRNA (siTCF4) or *LEF-1* siRNA (siLEF1) or combination of *TCF-4* and *LEF-1* siRNAs (siTCF4 + siLEF1) were treated with or without PGE2 (20 μg/mL) for 24 hours as indicated. Blots are representative of 3 independent experiments. Data represent means ± SD of 3 independent experiments. *, $P < 0.05$ and **, $P < 0.01$ by *t* test.

Published OnlineFirst November 13, 2012; DOI: 10.1158/0008-5472.CAN-12-2220

plasmids enhanced MIG-7 transcription and expression up to 4-fold in a dose-dependent manner (Fig. 3C). PGE2 increased transcription and expression of MIG-7 protein as well as β-catenin level (Fig. 3D and Supplementary Fig. S3B) up to 3-fold. The PGE-2-mediated increase of MIG-7 protein was attenuated partially (47%) by transfection with either *TCF-4* siRNA (siTCF4) or *LEF-1* siRNA (siLEF1) and abolished by combination of siTCF4 and siLEF1 (Supplementary Fig. S3B). These results suggest that PGE2 activates Akt/GSK-3β signaling to increase MIG-7 protein via enhancement of the β-catenin/LEF/TCF signaling cascade.

Elevation of MIG-7 protein level sustains phosphorylation of Akt, GSK-3β, and ERK1/2 via inactivating PP2A

To further understand why elevation of MIG-7 protein level may be pivotal for the effects on the COX-2/PGE2 and PI3K/Akt/GSK-3β signaling cascade, we undertook time-course analysis. Our results showed that in parental control cells or cells transfected only with scrambled siRNA control (siCont), PGE2 treatment increased phosphorylation of Akt, GSK-3β, and ERK1/2 by 4- to 6-fold within 1 hour, which then declined to the control level at 2 hours after treatment

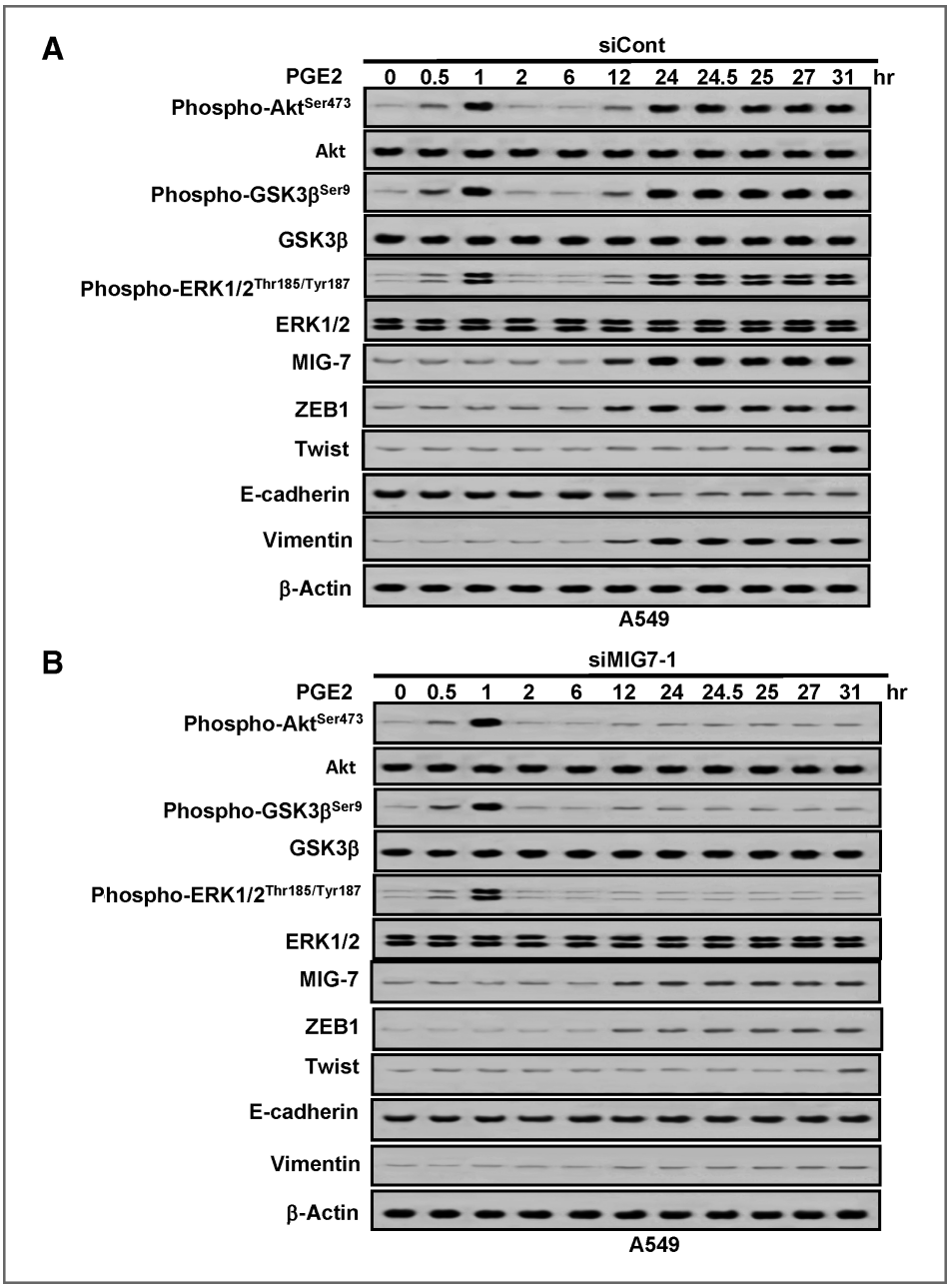

Figure 4. MIG-7 protein sustains phosphorylation of Akt and GSK-3β via inactivating PP2A in PGE2-treated cancer cells. A and B, lung cancer cells (A549) were transfected with scrambled siRNA (siCont) or *MIG-7* siRNA (siMIG7-1) for 48 hours and then treated with PGE2 (20 μg/mL) for various time as indicated. The treated cells were examined by immunoblotting. Blots are representative of 3 independent experiments.

Published OnlineFirst November 13, 2012; DOI: 10.1158/0008-5472.CAN-12-2220

(Fig. 4A and Supplementary Fig. S4A). MIG-7 protein level was not elevated until 12 hours after PGE2 treatment and reached a 4-fold plateau at 24 to 31 hours. After elevation of MIG-7 protein level, phosphorylation of Akt, GSK-3β, and ERK1/2 was increased again and sustained at significantly high levels (Fig. 4A and Supplementary Fig. S4A). In comparison, in MIG-7 knockdown cells, even though phosphorylation of Akt, GSK-3β, and ERK1/2 increased in 1 hour and declined to control level at 2 hours after PGE2 treatment in the same manner as control cells or siCont-transfected cells (Fig. 4B and Supplementary Fig. S4B), increase in MIG-7 protein level after 12 hours or later was attenuated and so was phosphorylation of Akt, GSK-3β, and ERK1/2 (Fig. 4B and Supplementary Fig. S4B).

Phosphorylation of Akt, GSK-3β, and ERK1/2 is negatively regulated by phosphatases, notably PP2A, which accounts for the majority of serine-threonine phosphatase activity in eukaryotic cells (30). We thus examined whether MIG-7 inactivates PP2A to sustain phosphorylation of Akt, GSK-3β, and ERK1/2. By using methods to determine the interaction of PP2A with Akt and assay the PP2A phosphatase activity (31), we found that in PGE2-treated cancer cells, the amount of Akt associated with PP2A regulatory unit B55-α and the phosphatase activity of PP2A were maintained at the same levels before the elevation of MIG-7 protein level (Supplementary Fig. S5A and S5B). Twelve hours after PGE2 treatment, the 2.5-fold increase in MIG-7 protein level was accompanied with a 55% decrease in PP2A activity and a 45% decline in the amount of Akt associated with B55-α (Supplementary Fig. S5A and S5B). Knockdown of MIG-7 in PGE2-treated cancer cells reversed the decline in the amount of Akt associated with B55-α and restored the activity of PP2A (Supplementary Fig. S5C and S5D).

Overexpression of MIG-7 increases anchorage-independent growth and invasive ability of lung cancer cells

Knockdown of MIG-7 in lung cancer cells attenuated COX-2/PGE2 and Akt-mediated EMT (Figs. 1C, 2C, 2D, and 4B, and Supplementary Fig. S1E and S4B), a central tumorigenic process related to cellular migration/invasion and metastasis (32). Our results showed that MIG-7 overexpression upregulated activities of migration and invasion and increased growth ability of lung cancer cells (A549, H1299, and CL1-0) in soft agar by 2-fold (Fig. 5A). Knockdown of MIG-7 with *MIG-7* siRNA (siMIG7-1 or siMIG7-2) in highly invasive CL1-5 human lung cancer cells decreased cell migration and invasion as well as clone-forming ability in soft agar by 40% to 55% (Fig. 5B). Similar effects of MIG-7 were confirmed in $A549^{EV\text{-}GL}$, $A549^{MIG7\text{-}GL}$, and $A549^{MIG7shMIG7\text{-}GL}$ as well as $CL1\text{-}0^{EV\text{-}GL}$, $CL1\text{-}0^{MIG7\text{-}GL}$ cells, and $CL1\text{-}0^{MIG7shMIG7\text{-}GL}$ lung cancer cells stably expressing EV, MIG-7 protein, *MIG7* shRNA, green fluorescent protein, and luciferase (GL; Fig. 5C and Supplementary Fig. S5E).

MIG-7 protein promotes lung cancer metastasis *in vivo*

To investigate whether MIG-7 is sufficient to induce lung cancer metastasis *in vivo*, we injected medium (vehicle), $A549^{EV\text{-}GL}$, $A549^{MIG7\text{-}GL}$, or $A549^{MIG7shMIG7\text{-}GL}$ cells, respectively, into the tail vein of a murine metastasis model. Our results showed that $A549^{MIG7\text{-}GL}$-bearing mice developed more number of tumor nodules (a 2.5-fold increase) in the lung compared with $A549^{EV\text{-}GL}$- and $A549^{MIG7shMIG7\text{-}GL}$-bearing mice on day 35 postinoculation (Fig. 6A and 6B). There was more Ki67-positive proliferating cells (a 2-fold increase) and larger tumor area in mice inoculated with $A549^{MIG7\text{-}GL}$ cells than in those inoculated with $A549^{EV\text{-}GL}$and $A549^{MIG7shMIG7\text{-}GL}$ cells (Fig. 6C). Analysis of lung tissue lysates showed that mice implanted with $A549^{MIG7\text{-}GL}$ cells had higher expression levels of MIG-7, ZEB1, Twist, and vimentin and lower expression level of E-cadherin (Fig. 6D) as compared with those implanted with $A549^{EV\text{-}GL}$ and $A549^{MIG7shMIG7\text{-}GL}$. The survival time of $A549^{MIG7\text{-}GL}$-bearing mice was significantly shortened than that of $A549^{EV\text{-}GL}$- and $A549^{MIG7shMIG7\text{-}GL}$-bearing mice (Fig. 6E; median survival time of 39.5 days versus 52 and 51.5 days, $P < 0.001$). Similar trends were found in comparing $CL1\text{-}0^{MIG7\text{-}GL}$- and $CL1\text{-}0^{MIG7shMIG7\text{-}GL}$-bearing mice (Supplementary Fig. S6A–S6D). Moreover, all the $CL1\text{-}0^{MIG7\text{-}GL}$-bearing mice perished before day 50 postinoculation; whereas all the mice inoculated with vehicle and $CL1\text{-}0^{EV\text{-}GL}$ as well as 5 of 6 mice inoculated with $CL1\text{-}0^{MIG7shMIG7\text{-}GL}$ survived even on day 70 postinoculation (Supplementary Fig. S6E). Stably silencing MIG-7 protein in CL1-5 cells ($CL1\text{-}5^{shMIG7\text{-}1}$ and $CL1\text{-}5^{shMIG7\text{-}2}$) by transfection with *MIG7-1* or *MIG7-2* shRNA also showed that downregulation of MIG-7 reduced *in vivo* lung metastasis of CL1-5 cells and prolonged survival time of tumor-bearing mice (Supplementary Fig. S7A–S7E).

MIG-7 protein level positively correlates with advanced stages of cancers in human lung tumor tissues

Analysis of MIG-7 protein levels in tumor and normal lung tissues of a human lung carcinoma TMA showed that the median MIG-7 protein level was higher in lung cancer (T) than normal (N) lung tissues ($P < 0.0001$); in locally advanced (T3 + T4) versus noninvasive or minimally advanced (T1 + T2) lung cancers ($P < 0.0001$); in cancers with lymph node involvement (N1 + N2 status) versus cancers without lymph node involvement (N0 status; $P < 0.0001$); and in stage II/III/IV versus stage I lung cancers ($P < 0.0001$; Fig. 7).

Discussion

Agonist of EP1 (ONO-DI-004) but not EP2, EP3 or EP4 was reported to increase invasion of hepatocellular carcinoma (HCC) (33). As PGE2 receptors transactivate epidermal growth factor receptor (EGFR) and mesenchymal-epithelial transition (MET), it has been proposed that there is a cross-talk between the COX-2/PGE2/EP1 and EGFR/c-Met signaling pathways that coordinately regulate human HCC cell invasion (33). In this study, we found, however, that the effects of COX-2 and PGE2 on EMT, MIG-7 protein level, MMP-2, and cancer cell migration/invasion were reversed by inhibition of EP4 (Fig. 2A, 2B, Supplementary Fig. S2B and S2C) but not EP1 or EP2. It remains to be elucidated whether these differences in EP4 and EP1 are due to different cell types and whether COX-2/PGE2/EP4 has any cross-talk with EGFR/c-Met signaling in lung cancer cells.

Published OnlineFirst November 13, 2012; DOI: 10.1158/0008-5472.CAN-12-2220

Although Twist has been shown to activate the Akt signaling pathway (34) and play an essential role in tumor metastasis (35), our time-course analysis of PGE2 effects showed that elevation of MIG-7 was associated with increase of EMT and phosphorylation of Akt, GSK-3β, and ERK, which occurred several hours before Twist induction (Fig. 4A and Supplementary Fig. S4). As variation in MIG-7 protein level did not affect COX-2 and PGE2 level (Fig. 1C and Supplementary S1E) and elevation in MIG-7 protein level by 2.5-fold was accompanied by a 55% decrease in the activity of PP2A (Supplementary Fig. S5A and S5B), a negative regulator of Akt phosphorylation, it is most likely that MIG-7 mediates sustainment of Akt, GSK-3β, and ERK1/2 phosphorylation primarily, if not exclusively, via this inactivating effect on PP2A. To what extent Twist and other phosphatases

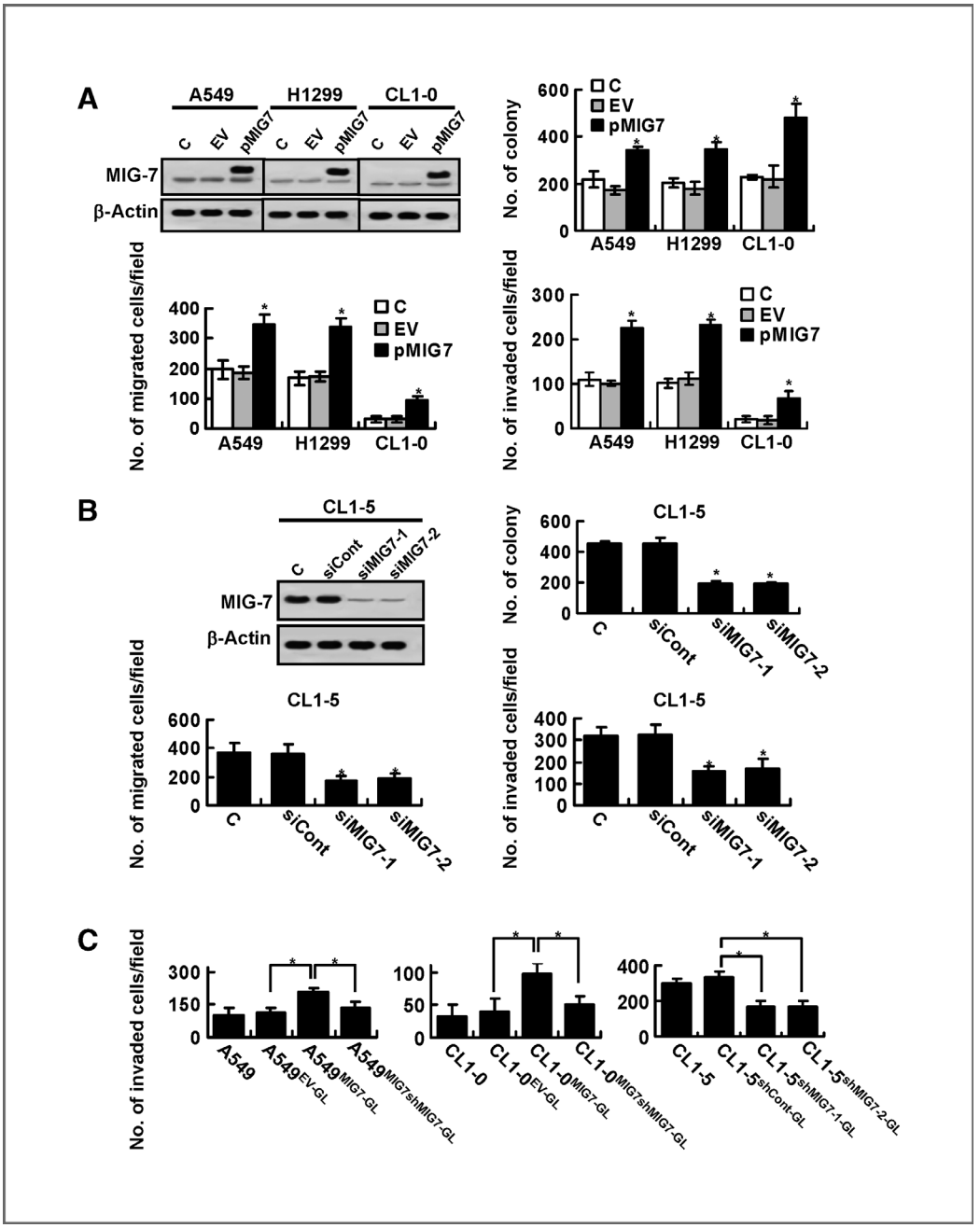

Figure 5. MIG-7 increases 3-dimensional growth and invasive ability of lung cancer cells. A and B, lung cancer cells (A549, H1299, and CL1-0; C) were transfected with EV, *MIG-7* plasmid (pMIG7), or control scrambled siRNA (-siCont), *MIG-7-1* siRNA(siMIG7-1), and *MIG-7-2* siRNA (siMIG7-2) as indicated. The transduced cells were examined by immunoblotting, anchorage-independent growth, migration, and invasion assays as described in Materials and Methods. C, the relative invasive ability of different stable cell lines were examined by invasion assay. Blots are representative of 3 independent experiments. Data represent means ± SD of 3 independent experiments. *, $P < 0.05$ by *t* test.

Published OnlineFirst November 13, 2012; DOI: 10.1158/0008-5472.CAN-12-2220

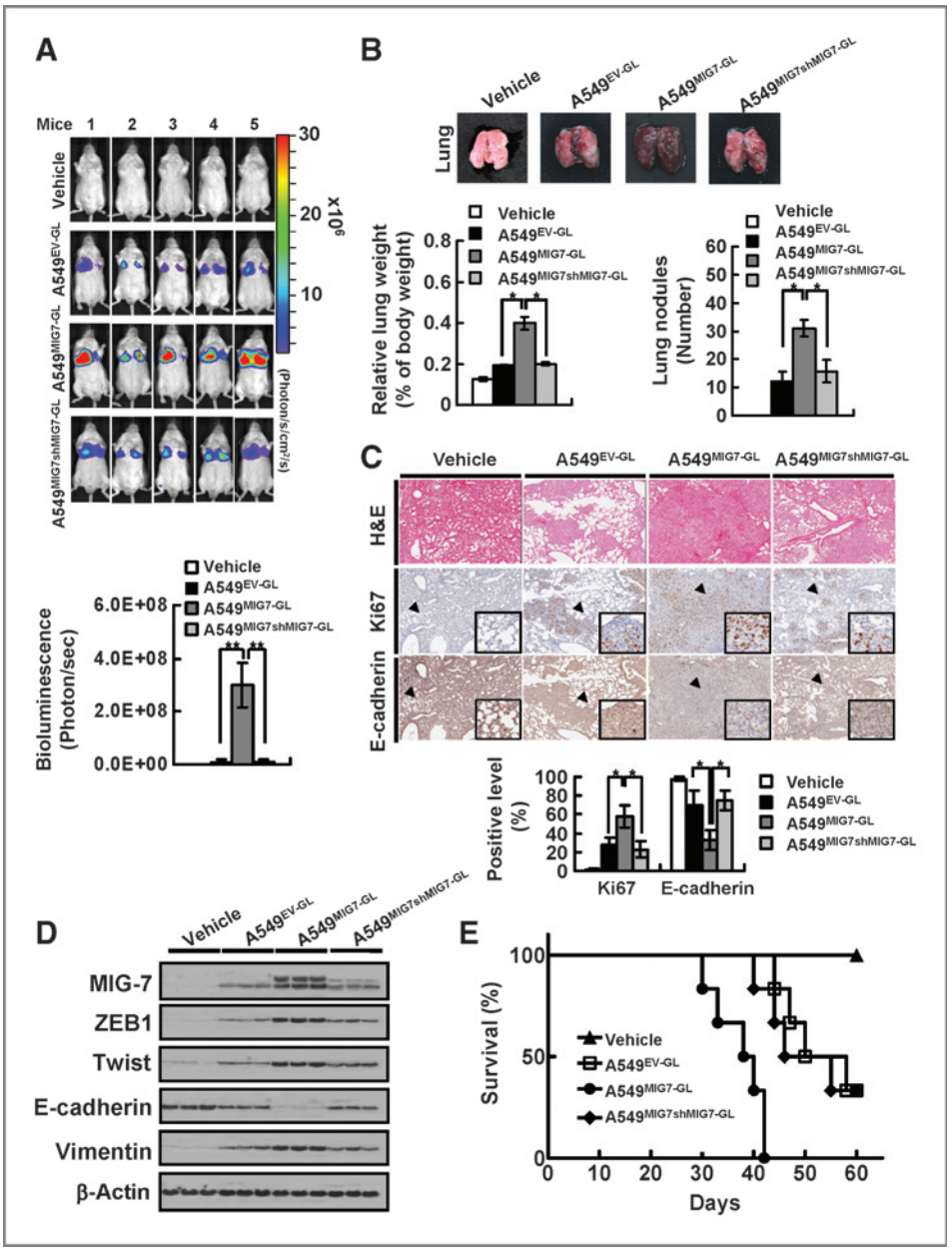

Figure 6. MIG-7 enhances lung cancer metastasis in an experimental murine metastasis model. $A549^{EV\text{-}GL}$, $A549^{MIG7\text{-}GL}$, and $A549^{MIG7shMIG7\text{-}GL}$ cells were generated as described in Materials and Methods and were injected into tail vein of mice (1×10^6/50 μL/mouse), respectively. Five weeks after cell implantation, bioluminescent images of whole body as well as H&E, immunohistochemical staining and cell lysates of lung were taken. A and B, the whole bodies of mice were detected by bioluminescent imaging and the lungs of mice were dissected from the surrounding tissue for weight and tumor nodule measurement. Data represent means ± SD of at least 3 mice of each group; *, $P < 0.05$; **, $P < 0.01$ by *t* test. C and D, the murine lung sections were analyzed after H&E (at ×40 magnification) and immunohistochemistry staining (at ×40 magnification; insets ×400 magnification) and cell lysates were extracted and analyzed by immunoblotting. Blots of 3 tissue samples of each group are representative of 3 independent experiments. E, percentage of survival in mice inoculated with $A549^{MIG7\text{-}GL}$ cells was compared with that in mice inoculated with $A549^{EV\text{-}GL}$ or $A549^{MIG7shMIG7\text{-}GL}$; $P < 0.001$, $n = 6$ by *t* test.

contribute to the PGE2-mediated phosphorylation of Akt, GSK-3β, and ERK1/2 remains to be elucidated.

MIG-7 activates MT1-MMP to regulate EMT and has been reported to be required for metastasis (19, 36–38). Our results show that MIG-7 protein facilitates EMT and metastasis of lung cancer cells resulting in the death of animals bearing these cancer cells (Fig. 5 and 6). As MT1-MMP regulates MMP-2 activation (39), it is likely that the increase of up to 2-fold MMP-2 activity by COX-2/PGE2 (Fig. 1D and Supplementary Fig. S1F) in lung cancer cells is at least in part through effect of MIG-7 on MT1-MMP.

In this study, we found that *siMIG7* reduced phosphorylation of serine 473 in Akt and Thr 185/Tyr 187 in ERK1/2 in lung cancer cells (Fig. 4). This result is consistent with the report of *MIG-7*-specific shRNA effects in endometrial carcinoma cell lines (19). Our finding of a positive correlation between MIG-7 protein level and malignant phenotypes and advanced stages of lung cancer (Fig. 7) is also consistent with that found in breast cancer tissue array (19).

Overexpressing and/or knockdown of MIG-7 in A549, CL1-0 and CL1-5 cells show that MIG-7 promotes lung cancer metastasis *in vivo* (Fig. 6, Supplementary Figs. S6 and S7). In addition, we have recently found that EMT and migration/invasion of other kinds of human cancers such as cervical HeLa cancer cells were promoted by overexpressing COX-2 and these effects of COX-2 were attenuated by 35% to 55% under MIG-7 knockdown. MIG-7 protein might thus

Published OnlineFirst November 13, 2012; DOI: 10.1158/0008-5472.CAN-12-2220

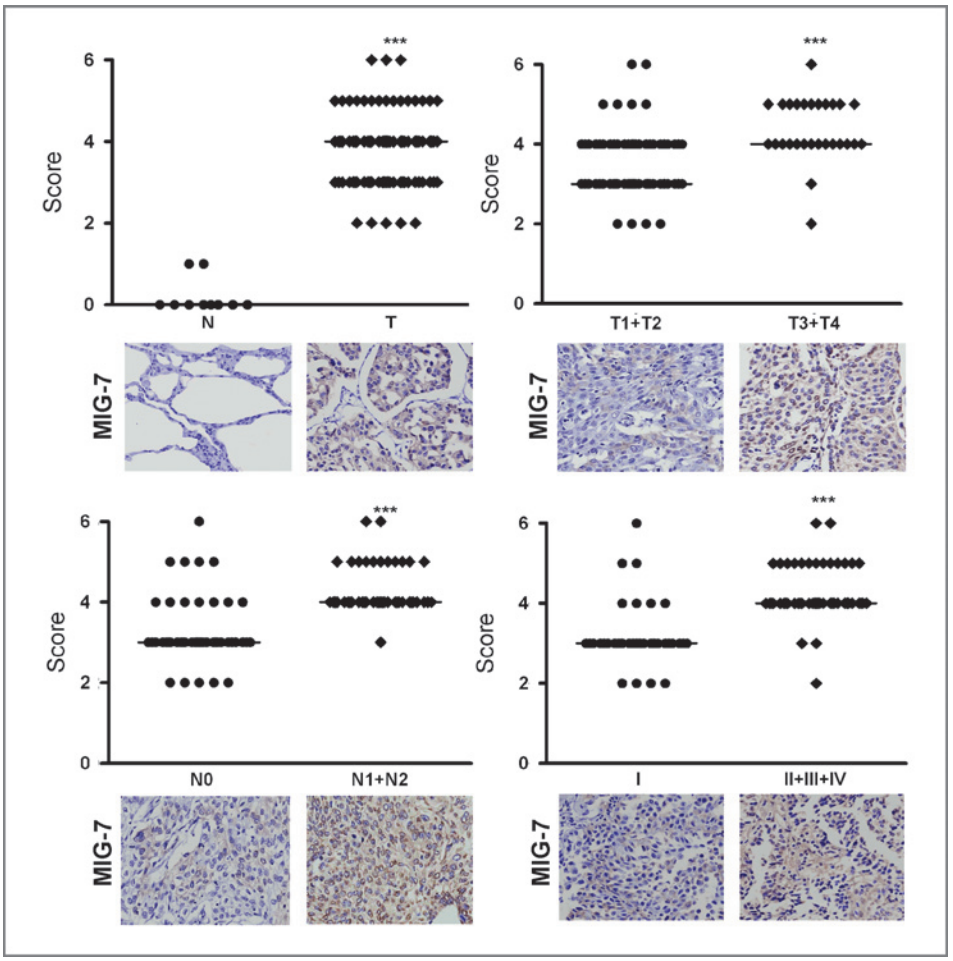

Figure 7. MIG-7 protein level positively correlates with advanced stages of cancers in human lung tumor tissues. Lung tissue sections from a human lung carcinoma microarray were analyzed by immunostaining with anti-MIG-7 antibodies. The percentage of positive cells and protein level of MIG-7 in each tissue sample were scored as described in Materials and Methods. More MIG-7 protein was found in cancers (T; $n = 89$) than normal tissues (N; $n = 10$); in advanced stage T3 + T4 cancers ($n = 28$) versus noninvasive or minimally advanced T1 + T2 cancers ($n = 61$); in cancers with lymph node involvement (N1 + N2; $n = 44$) versus those without lymph node involvement (N0; $n = 45$); and in stage II+III+IV ($n = 51$) versus stage I lung cancer ($n = 38$). The tissues and tumors were examined at ×200 magnification for MIG-7 immunostaining. Data are expressed as medians relative to each group of tissues; ***, $P < 0.0001$ by t test.

play an important role in invasion/metastasis of a variety of cancers.

As MIG-7 is rarely found in normal cells (Fig. 7 and Supplementary Fig. S1A; refs. 16–19) and change in MIG-7 level did not affect COX-2 and PGE2 level (Fig. 1C and Supplementary Fig. S1E), whereas, knockdown of MIG-7 attenuated the effects of COX-2/PGE2 and Akt signaling on EMT, MMP2, and cancer cell migration/invasion by 30% to 60% (Fig. 1C and D, 2C and D and Supplementary Fig. S1E and S1F), inhibiting metastatic cancer cells with MIG-7 inhibitors, *siMIG7*, or *MIG-7* shRNA might selectively block effects of COX-2/PGE2 and Akt/GSK-3β signaling thus inhibiting or reducing cancer cell invasion and metastasis without causing severe adverse effects on normal cells.

In summary, this report represents the first demonstration of a functional link between COX-2/PGE2, Akt/GSK-3β, β-catenin/LEF/TCF, MIG-7, and PP2A. These findings shed light on the mechanism of action of MIG-7 protein and suggest that MIG-7 may be an important therapeutic target for COX-2/PGE2- and Akt/GSK-3β-driven cancer metastasis

Disclosure of Potential Conflicts of Interest

No potential conflicts of interest were disclosed.

Authors' Contributions

Conception and design: M.-Y. Ho, S.-M. Liang, C.-M. Liang
Development of methodology: M.-Y. Ho, S.-W. Hung, C.-M. Liang
Acquisition of data (provided animals, acquired and managed patients, provided facilities, etc.): M.-Y. Ho, S.-M. Liang, S.-W. Hung, C.-M. Liang
Analysis and interpretation of data (e.g., statistical analysis, biostatistics, computational analysis): M.-Y. Ho, S.-M. Liang
Writing, review, and/or revision of the manuscript: M.-Y. Ho, S.-M. Liang, C.-M. Liang
Administrative, technical, or material support (i.e., reporting or organizing data, constructing databases): M.-Y. Ho, C.-M. Liang
Study supervision: S.-M. Liang, C.-M. Liang

Acknowledgments

The authors thank Dr. Wei-Hwa Lee for verifying the pathologic and clinical grade and tumor-node-metastasis classification of human lung carcinoma TMA and Dr. Michael Hsiao for offering the pCMV-GFP/luciferase-lentivirus. The authors also thank Ms. Tzu-Wen Tai for her assistance with flow cytometry analysis, and Ms. Miranda Loney for English editorial assistance.

Grant Support

This work was supported by Academia Sinica (S.-M. Liang and C.-M. Liang).

The costs of publication of this article were defrayed in part by the payment of page charges. This article must therefore be hereby marked *advertisement* in accordance with 18 U.S.C. Section 1734 solely to indicate this fact.

Received June 8, 2012; revised November 7, 2012; accepted November 9, 2012; published OnlineFirst November 13, 2012.

Published OnlineFirst November 13, 2012; DOI: 10.1158/0008-5472.CAN-12-2220

References

1. Fidler IJ. The pathogenesis of cancer metastasis: the 'seed and soil' hypothesis revisited. Nat Rev Cancer 2003;3:453–8.
2. Liotta LA, Stetler-Stevenson WG. Tumor invasion and metastasis: an imbalance of positive and negative regulation. Cancer Res 1991;51: 5054s–9s.
3. Sun S, Schiller JH, Spinola M, Minna JD. New molecularly targeted therapies for lung cancer. J Clin Invest 2007;117:2740–50.
4. Brown JR, DuBois RN. Cyclooxygenase as a target in lung cancer. Clin Cancer Res 2004;10:4266s–9s.
5. Castelao JE, Bart RD III, DiPerna CA, Sievers EM, Bremner RM. Lung cancer and cyclooxygenase-2. Ann Thorac Surg 2003;76:1327–35.
6. Hida T, Yatabe Y, Achiwa H, Muramatsu H, Kozaki K, Nakamura S, et al. Increased expression of cyclooxygenase 2 occurs frequently in human lung cancers, specifically in adenocarcinomas. Cancer Res 1998;58:3761–4.
7. Wolff H, Saukkonen K, Anttila S, Karjalainen A, Vainio H, Ristimaki A. Expression of cyclooxygenase-2 in human lung carcinoma. Cancer Res 1998;58:4997–5001.
8. Chell S, Kaidi A, Williams AC, Paraskeva C. Mediators of PGE2 synthesis and signalling downstream of COX-2 represent potential targets for the prevention/treatment of colorectal cancer. Biochim Biophys Acta 2006;1766:104–19.
9. Wang D, Dubois RN. Eicosanoids and cancer. Nat Rev Cancer 2010; 10:181–93.
10. Fresno Vara JA, Casado E, de Castro J, Cejas P, Belda-Iniesta C, Gonzalez-Baron M. PI3K/Akt signalling pathway and cancer. Cancer Treat Rev 2004;30:193–204.
11. Hanada M, Feng J, Hemmings BA. Structure, regulation and function of PKB/AKT–a major therapeutic target. Biochim Biophys Acta 2004;1697:3–16.
12. Mukherjee D, Nissen SE, Topol EJ. Risk of cardiovascular events associated with selective COX-2 inhibitors. JAMA 2001;286:954–9.
13. Yun J. Allosteric AKT inhibitors as a targeted cancer therapy. Cancer Biol Ther 2010;9:504–6.
14. Vanchieri C. Vioxx withdrawal alarms cancer prevention researchers. J Natl Cancer Inst 2004;96:1734–5.
15. Zhang J, Ding EL, Song Y. Adverse effects of cyclooxygenase 2 inhibitors on renal and arrhythmia events: meta-analysis of randomized trials. JAMA 2006;296:1619–32.
16. Crouch S, Spidel CS, Lindsey JS. HGF and ligation of alphavbeta5 integrin induce a novel, cancer cell-specific gene expression required for cell scattering. Exp Cell Res 2004;292:274–87.
17. Petty AP, Garman KL, Winn VD, Spidel CM, Lindsey JS. Overexpression of carcinoma and embryonic cytotrophoblast cell-specific Mig-7 induces invasion and vessel-like structure formation. Am J Pathol 2007;170:1763–80.
18. Phillips TM, Lindsey JS. Carcinoma cell-specific Mig-7: a new potential marker for circulating and migrating cancer cells. Oncol Rep 2005;13: 37–44.
19. Petty AP, Wright SE, Rewers-Felkins KA, Yenderrozos MA, Vorderstrasse BA, Lindsey JS. Targeting migration inducting gene-7 inhibits carcinoma cell invasion, early primary tumor growth, and stimulates monocyte oncolytic activity. Mol Cancer Ther 2009;8:2412–23.
20. Chu YW, Yang PC, Yang SC, Shyu YC, Hendrix MJ, Wu R, et al. Selection of invasive and metastatic subpopulations from a human lung adenocarcinoma cell line. Am J Respir Cell Mol Biol 1997;17:353–60.
21. Chen TA, Wang JL, Hung SW, Chu CL, Cheng YC, Liang SM. Recombinant VP1, an Akt inhibitor, suppresses progression of hepatocellular carcinoma by inducing apoptosis and modulation of CCL2 production. PLoS One 2011;6:e23317.
22. Peng JM, Chen YH, Hung SW, Chiu CF, Ho MY, Lee YJ, et al. Recombinant viral protein promotes apoptosis and suppresses invasion of ovarian adenocarcinoma cells by targeting alpha5beta1 integrin to down-regulate Akt and MMP-2. Br J Pharmacol 2012;165:479–93.
23. Ho MY, Leu SJ, Sun GH, Tao MH, Tang SJ, Sun KH. IL-27 directly restrains lung tumorigenicity by suppressing cyclooxygenase-2-mediated activities. J Immunol 2009;183:6217–26.
24. Chiu CF, Ho MY, Peng JM, Hung SW, Lee WH, Liang CM, et al. Raf activation by Ras and promotion of cellular metastasis require phosphorylation of prohibitin in the raft domain of the plasma membrane. Oncogene 2012 Mar 12. [Epub ahead of print].
25. Sheng H, Shao J, Washington MK, DuBois RN. Prostaglandin E2 increases growth and motility of colorectal carcinoma cells. J Biol Chem 2001;276:18075–81.
26. Buchanan FG, DuBois RN. Connecting COX-2 and Wnt in cancer. Cancer Cell 2006;9:6–8.
27. Dar AA, Belkhiri A, El-Rifai W. The aurora kinase A regulates GSK-3beta in gastric cancer cells. Oncogene 2009;28:866–75.
28. Shao J, Jung C, Liu C, Sheng H. Prostaglandin E2 Stimulates the beta-catenin/T cell factor-dependent transcription in colon cancer. J Biol Chem 2005;280:26565–72.
29. Ma C, Wang J, Gao Y, Gao TW, Chen G, Bower KA, et al. The role of glycogen synthase kinase 3 beta in the transformation of epidermal cells. Cancer Res 2007;67:7756–64.
30. Westermarck J, Hahn WC. Multiple pathways regulated by the tumor suppressor PP2A in transformation. Trends Mol Med 2008;14:152–60.
31. Kuo YC, Huang KY, Yang CH, Yang YS, Lee WY, Chiang CW. Regulation of phosphorylation of Thr-308 of Akt, cell proliferation, and survival by the B55alpha regulatory subunit targeting of the protein phosphatase 2A holoenzyme to Akt. J Biol Chem 2008;283:1882–92.
32. Thiery JP, Sleeman JP. Complex networks orchestrate epithelial-mesenchymal transitions. Nat Rev Mol Cell Biol 2006;7:131–42.
33. Han C, Michalopoulos GK, Wu T. Prostaglandin E2 receptor EP1 transactivates EGFR/MET receptor tyrosine kinases and enhances invasiveness in human hepatocellular carcinoma cells. J Cell Physiol 2006;207:261–70.
34. Li J, Zhou BP. Activation of beta-catenin and Akt pathways by Twist are critical for the maintenance of EMT associated cancer stem cell-like characters. BMC Cancer 2011;11:49.
35. Yang J, Mani SA, Donaher JL, Ramaswamy S, Itzykson RA, Come C, et al. Twist, a master regulator of morphogenesis, plays an essential role in tumor metastasis. Cell 2004;117:927–39.
36. Koshikawa N, Minegishi T, Sharabi A, Quaranta V, Seiki M. Membrane-type matrix metalloproteinase-1 (MT1-MMP) is a processing enzyme for human laminin gamma 2 chain. J Biol Chem 2005;280:88–93.
37. Koshikawa N, Giannelli G, Cirulli V, Miyazaki K, Quaranta V. Role of cell surface metalloprotease MT1-MMP in epithelial cell migration over laminin-5. J Cell Biol 2000;148:615–24.
38. Hotary KB, Allen ED, Brooks PC, Datta NS, Long MW, Weiss SJ. Membrane type I matrix metalloproteinase usurps tumor growth control imposed by the three-dimensional extracellular matrix. Cell 2003; 114:33–45.
39. Lehti K, Lohi J, Valtanen H, Keski-Oja J. Proteolytic processing of membrane-type-1 matrix metalloproteinase is associated with gelatinase A activation at the cell surface. Biochem J 1998;334 (Pt 2): 345–53.

Cancer Research
The Journal of Cancer Research (1916–1930) | The American Journal of Cancer (1931–1940)

AACR American Association for Cancer Research

MIG-7 Controls COX-2/PGE2-Mediated Lung Cancer Metastasis

Ming-Yi Ho, Shu-Mei Liang, Shao-Wen Hung, et al.

Cancer Res Published OnlineFirst November 13, 2012.